EFFECT OF LOADING TYPE ON RC T-BEAM SECTIONS INVOLVING CONSTRUCTION ERRORS

El-Said A. Bayoumi[a*]

Abstract: The paper presents the effect of loading type on RC T-beam sections involving construction errors. This study involved 12 RC T- beams specimens divided into two main categories according to loading method. First category was loaded with uniformly distributed load at two-edges of slab while the second, were loaded with two-point concentrated loads at the middle length of beam specimen. The aim of this study is to evaluate, the effect of malposition of slab reinforcement, unequal configuration of slab reinforcement and change in bar diameter of slab reinforcement on the structural behavior of T-beam sections. The results indicated that malposition of slab reinforcement leads to a lower bending moment capacity of the slab. Flexural capacity of T-beams was higher than the rectangular beams where part of slab contributes to the resistance of the loads. Well-arranged distribution of reinforcement improves the ductile behavior of the slab and reduces the corresponding deflections.

INTRODUCTION

There are many projects are being implemented all over the world. Some of the projects involve the construction of buildings. Nevertheless, some of the buildings are poorly constructed and maintained. The concrete structure needs to be inspected and maintained regularly. In the last few years, a number of concrete buildings collapsed in the world under apparent normal circumstances. These failures are pre-dominantly due to human errors within the design or during construction of these buildings. Cracks in concrete may affect appearance only or may indicate significant structural distress or a lack of durability. Cracks may represent the total extent of the damage or may point to problems of greater magnitude. Their significance depends on the type of structure, as well as the nature of cracking [1-3].

Few investigations have addressed the shortcomings which frequently existed in the execution and cracking in reinforced concrete (RC) structures. These defects can be classified into two main categories; the first category focuses on the defects that occur in the detailing of reinforcing bars and cracking in RC elements, while the other category focuses on the strength of concrete [4-6]. In Egypt, Housing and Building National Research Center (HBNRC) has conducted a statistical study on the causes of deterioration in concrete structures in different periods. This statistical study illustrated that about 83% of the causes of damage were referred to bad execution practices starting from the eighties of the past century. Thus, there is an increasing demand for developing a better understanding of the effect of bad execution practices on the performance of concrete structures, especially on cracking in order to determine the proper method of repairing these defects [7-9].

Reinforced concrete (RC) structures consist of a series of members. The flooring of buildings have a slab-and-beam system, in which the slab spans between beams, which in turn applies loads to columns and the column loads are applied to footings, which distribute the load over a sufficient area of soil. Most of the reinforced concrete systems are cast monolithic. During construction, concrete from the bottom of the deepest beam to the top of slab, is placed at once. Therefore the slab serves as the top flange of the beams. The concrete slabs and beams act together in resisting the applied loads. As a result, the beam will have an extension concrete part at the top called flange and the portion of the beam below the slab is called the web. To consider a slab and a beam as a T-section, it is necessary to ensure interaction between these elements by a solid connection. Connection in the contact between the slab and the beam must be capable of ensuring a proper resistance to longitudinal and transverse flexural forces. T-section beams with the advantages of easy construction and saving costs have been extensively used in the design of flooring systems and are still in use as an economic and efficient construction system [10-12].

An experimental investigation was carried out to investigate the serviceability behavior of normal strength concrete (NSC) and high strength concrete (HSC) T-beams by I. Shaaban et al. (2017). They studied the effect of flange dimensions (breadth and thickness) on the crack pattern. The load-deflection response was evaluated experimentally for 10 beams comprising of the two studied groups viz. NSC and HSC T-beams. It was found that an increase in the flange dimensions (breadth and thickness) delayed the cracks initiation, its propagation and increased the maximum applied load prior to failure, and reduced the short term deflection of the beams. Prior to failure, the increment in the maximum loads was up to 22% while the deflection reduced by 31% for NSC and 23% for HSC beams [13 and 14].

R. Thamrin et al. (2016) [15] investigated shear strength of reinforced concrete T-beams without stirrups. The test variables were type of beam cross section and ratio of longitudinal reinforcement. Six simply supported beams, consisting of three beams with rectangular cross section and three beams with T section, subjected to two point load were tested until failure. They concluded that shear capacity of T-beams was higher than rectangular beams, with the values ranging from 5 to 25%, depending on the ratio of longitudinal reinforcement which influences the shear

[a]Department of Civil Engineering, Qassim University, Engineering College, Buraydah 52571, Saudi Arabia. Corresponding author email address: saidbay80@hotmail.com

Loading Type	Group	Specimen ID	Notes
Loading slab only (uniform distributed loads at the two-edges of slab)	Malposition of slab reinforcement (GIM)	GIM-1 (Control)	$(t_{mis.}/t_s) = 20\%$
		GIM-2	$(t_{mis.}/t_s) = 40\%$
		GIM-3	$(t_{mis.}/t_s) = 60\%$
		GIM-4	$(t_{mis.}/t_s) = 80\%$
	Effect of unequal configuration of slab reinforcement (GIIA)	GIIA-1	——
		GIIA-2	——
	Effect of change in bar diameter of slab reinforcement (GIIID)	GIIID-1	Slab reinforcement = 11Ø6/m
		GIIID-2	Slab reinforcement = 4Ø10/m
Loading slab and beam simultaneously with concentrated loads	Malposition of slab reinforcement (GIM)	M-1	$(t_{mis.}/t_s) = 20\%$
		GIM-5	$(t_s) = 0\%$
	Effect of unequal configuration of slab reinforcement	A-1	——
	Effect of change in bar diameter of slab reinforcement	D-2	Slab reinforcement = 4Ø10/m

capacity of the beam as well as the angle of diagonal shear crack.

A number of researchers conducted studies on the shear strength behavior of the reinforced concrete T-beams. They found that a web reinforced shear critical reinforced concrete T-beam subjected to a concentrated point load will fail by one of two mechanisms. The first is a beam shear mechanism in which a diagonal tension crack continues from the web and penetrates into the flange. While the second is a punching shear mechanism whereby the applied load punches through the flange. An increase in the ratio of flange width to web width is shown to produce an accompanying increase in the ultimate strength of a reinforced concrete T-beam, provided the ratio of flange depth to an effective depth is above a particular minimum value. This increase in shear resistance with an increase in the ratio of flange width to web width continues until the flange is wide enough to allow the formation of a failure mechanism whereby the load point punches through the flange. The existence of slab contributed to increase the shear resistance in the T-beams, where the shear failure loads increase by 42% of rectangular section in the T-beams without stirrups and ratio up to 43% in the T-beams with ordinary web stirrups while the ratio up to 54% in the T-

beams with flange stirrups [16]. The shear resistance increases with the increase of slab thickness. When the ratio of slab thickness to beam thickness increase from 13% to 27% the shear failure loads increase by ratio 45%. Increases in the flange width of a T-beam give higher shear capacity with a nonlinear relationship for the T-beam with shear reinforcement [17-19].

EXPERIMENTAL PROGRAM

A. DETAILS OF SPECIMEN

The main objective of the experimental program was to investigate the structural behavior due to change in position and ratio of negative reinforcement in the concrete slabs and attached beams. The experimental program was divided into two main categories according to the loading type where specimens of the first category were loaded on the slab only with uniformly distributed load at two-edges of slab. A total of eight specimens were prepared for this type. While the second category consisted of four specimens where the specimens were loaded on the slab and beam simultaneously. T-beams and rectangular beams were tested under mid-span two-concentrated loads at 1/3 and 2/3 of the span of the beam.
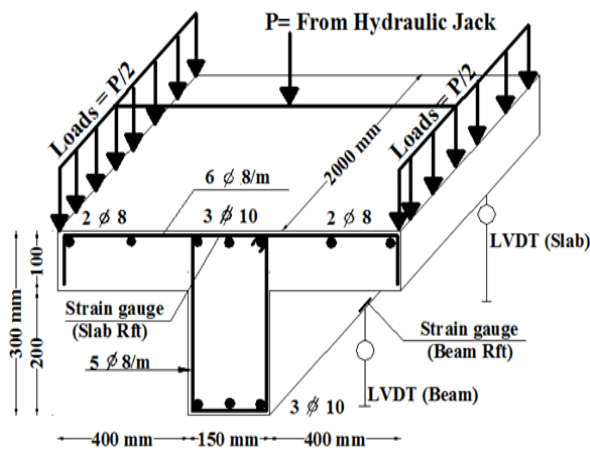
(a)

(b)

Figure 1 (a) specimen details and (b) uniform distributed loads at the two-edges

(a)

(b)   (c)
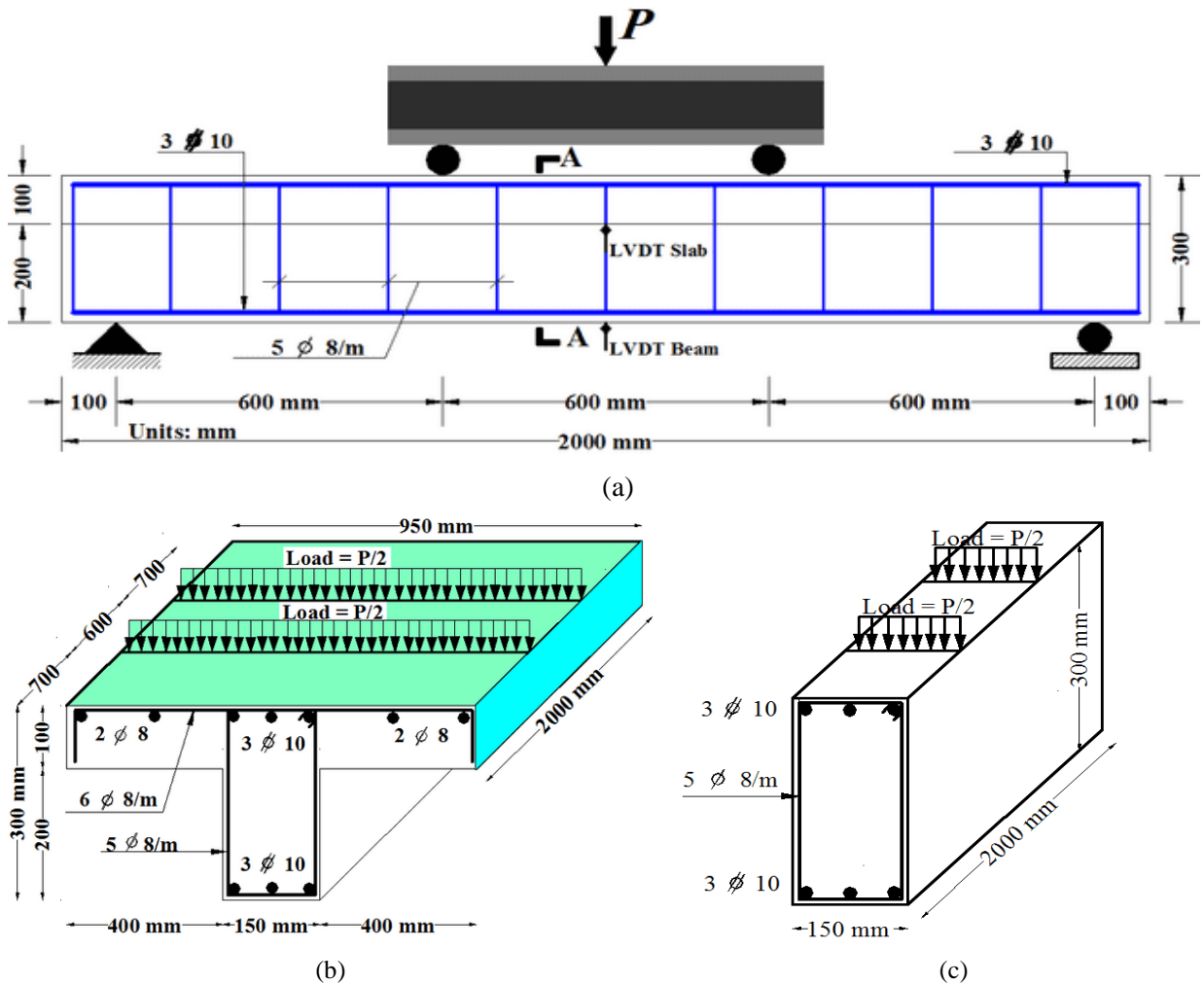
Figure 2 Loading of slab and beam simultaneously with two concentrated loads (a) Layout of reinforcement and test setup of two-point loading (b) A-A section for T-beam (c). Rectangular section

The experimental work involved casting and testing of 10 simply supported RC T beam, in addition one rectangular beam specimen. The dimensions of T-beam specimens used in this investigation were 150mm×200mm×2000mm in web-width, depth and length, respectively. The thickness and width of the flange of the T-section beam are 100mm and 950mm, respectively. While the dimensions of rectangular beam were length 2000mm, width 150mm and thickness 300mm. Figure 1, Figure 2 and Table 1 show the details of specimens.

All the T-section beams were simply supported with a clear span of 1800mm. Two types of steel reinforcement were used in fabricating T-beam sections. Reinforcement of

the flange (slab) and the stirrups of the projected beam (web) were mild-steel (yield strength of 240MPa), and all the projected beams were reinforced with 3 Φ10 bars as a main (bottom) and a secondary (top) reinforcement (high-grade steel with yield strength of 360MPa). The modulus of elasticity for steel reinforcement was considered as Es=210GPa. The vertical stirrups reinforcement was 8mm diameter spaced at 200mm acting as transverse reinforcement. The reinforcement of the slab was changed from specimen to specimen according to the type of parameter.

B. DETAILS OF EXPERIMENTAL PARAMETERS
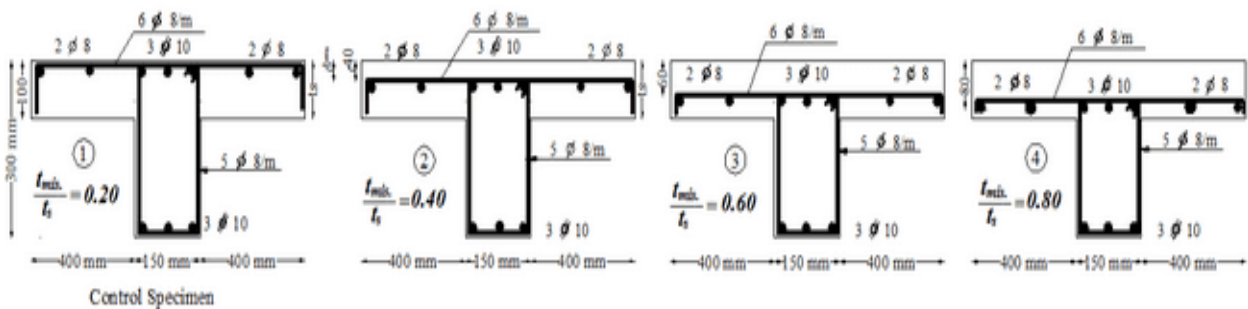
Figure 3 Specimens of first parameter
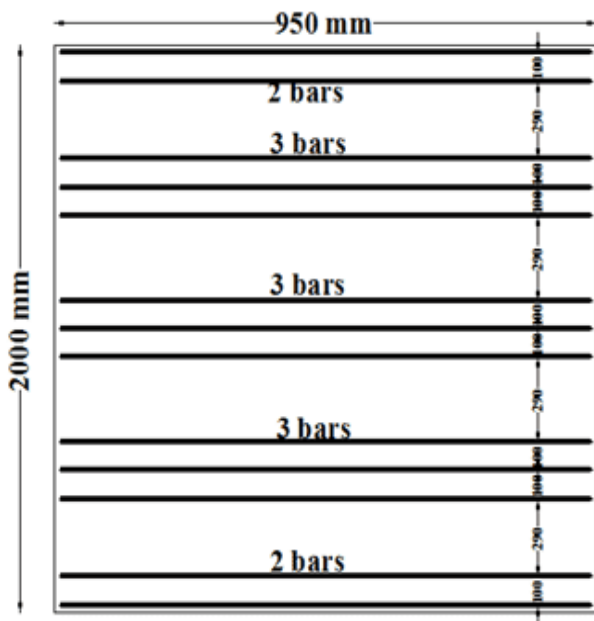
Figure 4 Plan of specimen GIIA-1
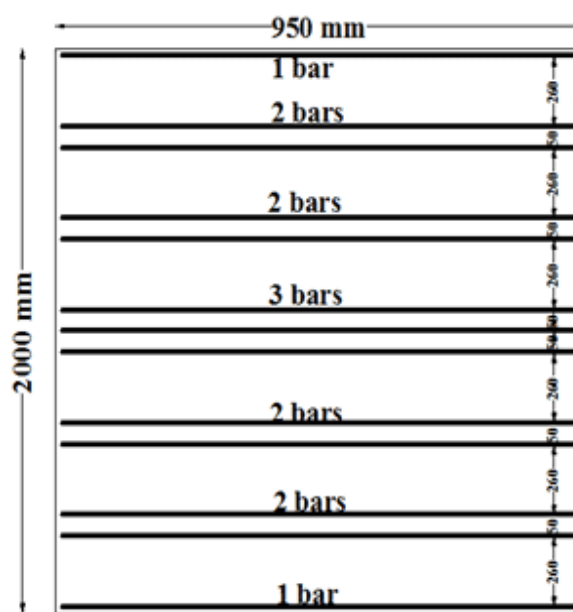
Figure 5 Plan of specimen GIIA-2

The specimens were subjected to uniform distributed loads at two-ends of slab and were divided into three parameters. The first parameter discussed the impact of malposition of slab reinforcement, the second parameter investigated the effect of unequal configuration of slab reinforcement while the last parameter examined the effect of a change in bar diameter of slab reinforcement on the efficiency of whole T-beam sections.

The first parameter consisted of four specimens, GIM-1 (control), GIM-2, GIM-3, and GIM-4, as shown in Figure 3. The variable of all these specimens was the depth of slab reinforcement. The malposition of slab reinforcement was $(t_{mis.}/t_s)$ varied as 0.2, 0.4, 0.6 and 0.8, percent respectively where $t_{mis.}$ is the misplacement of slab reinforcement while t_s is the thickness of slab. Control specimen (GIM-1) was made with standard requirements of good compaction using a mechanical vibrator, enough concrete cover, well-arranged reinforcement. No splices in the reinforcement of slab or beam were used in this control specimen. All specimens were constructed in the laboratory at Faculty of Engineering, AL-Azhar University.

While the second parameter contained two specimens, in addition to the control specimen. In this group, eccentricity of the main steel in slab was the major parameter. The area of steel for slab was constant (13Ø8mm on the length of the slab), but the distribution of steel was varied for two specimens (unequal distribution of slab reinforcement).

In first specimen (GIIA-1), unequal arrangement of slab reinforcement was used with three reinforcement bars at the mid-span of the slab at 50mm while two bars were placed at the distance of 260mm from two sides from the previous three bars keeping the distance between these bars as 50 mm. Moreover, there are two bars from two sides at the distance of 260 mm from the end of the slab. At the ends of the specimen one bar was erected. Figure 4 illustrates plan of reinforcement distribution of slab specimen (GIIA-1). In another specimen (GIIA-2), the eccentricity of slab reinforcement was in three groups, every group comprises three bars, and there are two distances between three bars.

This distance was 100 mm while the distance between groups was 290 mm. At the end of the specimen, two bars were erected from two sides, and the distance was 100 mm. Plan of slab reinforcement distribution for specimen (GIIA-2) is shown in Figure 5.

The last parameter comprised of three specimens (GIIID-1), (GIIID-2), in addition to the control specimen GIM-1, and identifies the change in bar diameter of slab reinforcement. The ratio of steel was not changed but the diameter only was changed. The first specimen was of the diameter 6mm whereas the diameter of 10mm was used in the second specimen. In the first specimen (GIIID-1), the area of steel was fulfilled by 11Ø6/m while the second specimen (GIIID-2) comprise 4Ø10/m.

However, the remaining specimens in this research were subjected to two-concentrated loads affected on slab and beam simultaneously. Total 3 T-section beams are prepared, in addition to one specimen (rectangular beam). Thus, one specimen; namely, M-1 investigated the impact of malposition of slab reinforcement with details of reinforcement of this specimen similar to specimen GIM-1 while the specimen GIM-5 was designed so that the section was a rectangular section without slab to identify the performance of slab in load resistance. One specimen studied the effect of irregular arrangement of slab reinforcement on the behavior of whole T-beam sections. This specimen was namely A-1 and the details of reinforcement were same like the previous specimen GIIA-1. One specimen namely D-2 displayed the effect of change in bar diameter of slab reinforcement and this specimen was similar to the previous specimen GIIID-2.

C. MATERIALS AND METHODS

The materials used in casting of the reinforced concrete specimens are Ordinary Portland cement (Type I), natural clean sand (fine aggregates); crushed stone (coarse aggregate) and clean drinking fresh water free from impurities. The concrete mix used in all experimental specimens was designed according to the Egyptian code of practice. The concrete mix was designed to obtain a target

Figure 6 Cracks pattern of specimen GIM-1

Figure 7 Cracks pattern of specimen GIM-2

Figure 8 Cracks pattern of specimen GIM-3

Figure 9 Cracks pattern of specimen GIM-4

strength of 25 MPa at the age of 28 days for all specimens. Mix proportions by weight (kg/m^3) are presented in Table 2.

Table 2 Concrete Mix Proportions

Constituents	Proportions, *Kg/m³*
Crushed stone	1256
Gradate sand	628
Cement	350
Water	175

All specimens were cast in plywood formwork simultaneously and cured under moist gunny. Plywood formwork were removed after 48 hrs. From casting, then the specimens were covered with wet burlap, and stored under laboratory conditions for 28 days. In addition, to determine the compressive strength of concrete after 7 and 28 days from the pouring of concrete, 18 standard cube tests $150 \times 150 \times 150 mm^3$ were also cast; 9 concrete cubes were tested after 7 days and the remaining cubes were tested after 28 days. All specimens were casted from the same concrete mix for which the average compressive strength was 23.44 MPa at 7 days, while at 28 days was equal to 29.76 MPa.

D. TEST SETUP AND INSTRUMENTATION DETAILS

The tests were carried out in a 100-ton universal testing machine. Each T-beam section was tested as a simply supported beam by using a vertical hydraulic jack. Linear varying displacement transducers (LVDTs) were installed at the mid-span of slab and beam to record the central deflections of the slab and the beam at different loading levels. In order to measure the strain distribution along the cross-section of the T-section beam, two linear strain gauges were installed on the main flexural reinforcing bars in the slab and the beam at mid-span of the specimen to record the strains developed in the reinforcements during the testing process. All T-beam sections were tested during loads and the LVDTs were removed before the failure load occurred. Cracks were detected through visual observation during the testing of all specimens, as well as marking the propagation of cracks at each load increment. The cracking and ultimate loads were accurately recorded during each test.

Results And Discussion for Loading Slab with Uniform Distributed Loads At The Two-Edges Of Slab

A. CRACK PATTERN AND FAILURE MECHANISM FOR SPECIMENS OF PHASE I

For Specimens GIM: Figure 6 shows the pattern of cracks for control specimen GIM-1. The first visible crack was initiated in the border line between slab (flange) and beam (web) at load equal to 10kN on both sides of the beam. These cracks were started in the region of the maximum tensile stress in the slab. These cracks extended on the boundary between the slab and the beam along the entire

Figure 10. Cracks pattern of specimen GIIA-1

Figure 11. Cracks pattern of specimen GIIA-2

Figure 12. Cracks pattern of specimen GIIID-1

Figure 13. Cracks pattern of specimen GIIID-2

length of the specimen. Then, by increasing the applied load, the cracks grow wider and deeper until the failure of the slab. The failure was flexural failure and the ultimate load was about 32kN.

For the remaining specimens of GIM, it was observed that the cracks were initiated at one side of border line between slab (flange) and beam (web) spread along the length of specimen. These cracks were extended along the overall length of the specimens and occurred due to slabs maximum bending moment. The loads at the initial cracks were about 5kN, 4.5kN and 4kN for specimens GIM-2, GIM-3 and GIM-4, respectively. At the failure of these specimens, the width of the cracks was noticeably widened and highly propagated at the face of the intersection between slab and beam where the height of reinforcement in slab reduced. The specimens were failed when the applied loads reached about 25kN, 20.5kN and 18.5kN for specimens GIM-2, GIM-3 and GIM-4, respectively. It was noticed that; the specimens were suddenly failed. This may due to the malposition of slab reinforcement, especially in specimens GIM-3 and GIM-4, where (t_{mis}/t_s) of these specimens were 0.6 and 0.8 respectively. Figures 7, 8 and 9 show the photo of specimens GIM-2, GIM-3, and GIM-4, respectively after the failure.

For Specimens GIIA: The specimens GIIA-1 and GIIA-2 exhibited basically the same cracking pattern and final mode of failure in nature of loading. The failure of the specimens was flexural tensile failure in the slab at the interface lines between the slab and attached beam. Also, the cracks were started in the region where there was no

reinforcing bars in the slab and propagated towards the loading points. The first crack was initiated at loads of about 7.5kN and 12kN for specimens GIIA-1 and GIIA-2, respectively. In case of specimen GIIA-1, horizontal cracks appeared in slab at early loading levels and inclined towards the loading lines, especially, were spread in the zones where there was no main reinforcement in the slab. This may be due to the improper rebar spacing of slab reinforcement. As the load was further increased, the crack became wider and extended at both sides of the beam on the overall length of specimen up to failure. The specimens GIIA-1 and GIIA-2 were failed at loads of about 28kN and 30.5kN, respectively. The unequal distribution of slab reinforcing steel in the negative moment zones resulted in improper slab resistance to the loads. The cracking patterns of tested specimens GIIA-1 and GIIA-2 at failure are shown in Figures 10 and 11, respectively.

For Specimens GIIID: The cracks patterns for specimens GIIID-1 and GIIID-2 are depicted in Figures 12 and 13, respectively. The first cracks were longitudinal flexural cracks in the vicinity of the tension zone within and near the maximum moment region at the connection of slab (web) with beam (flange) at a load of about 4.60kN and 7kN for specimens GIIID-1 and GIIID-2, respectively. These cracks were continued on the overall length of specimen.

For specimen GIIID-1, at higher loading stages, the rate of formation of new cracks significantly decreased. Moreover, the existing cracks grow wider, especially the initial formed cracks. The specimen failed at ultimate load of about 19kN in the region of maximum negative moment

Table 3. Summary of the results for tested specimens of loading slab only

Loading Type	Specimen Notation	Cracking Load (P_{cr})(kN)	Ultimate Load (P_u) (kN)	Ultimate deflection Δ_u (mm)	$\dfrac{P_{cr}}{P_u}$	$\dfrac{P_u}{P_u \text{ (Control)}}$	Toughness (kN.mm)
Loading slab only (uniform distributed loads at the two-edges of slab)	GIM-1 (Control)	10	32	35	0.31	1	981.213
	GIM-2	5	25	31	0.2	0.781	701.81
	GIM-3	4.5	20.5	32	0.22	0.64	589.82
	GIM-4	4	18.5	34	0.32	0.578	496.95
	GIIA-1	7.5	28	33	0.24	0.875	828.088
	GIIA-2	12	30.5	36.8	0.42	0.953	973.09
	GIIID-1	4.6	19	44.5	0.24	0.593	606.64
	GIIID-2	7	38	44	0.18	1.187	1412.71

affecting on T-beam section. Before failure, diagonal crack was appeared and propagated toward the connection of the beam to the slab and continued in the slab in the direction of loading. Although this specimen failed at a lower loading value, tension reinforcement of the slab was yielded, indicating that 6mm diameter reinforcement was weak in load resistance. For specimen GIIID-2, with the increase in load, cracks were appeared at the borderline between the beam and the slab. The width of the cracks was increased with the increase in the loading up to ultimate load at load of about 38kN. This specimen exhibited a high resistance to the loads compared with specimens GIM-1 and GIIID-1.
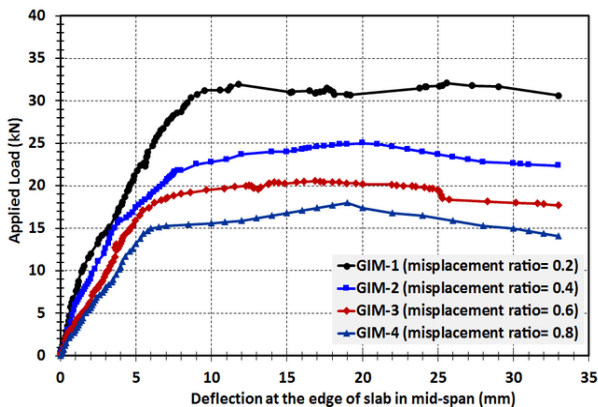
Figure 14 Comparison between the tested specimens of group GIM

Load-Deflection Behavior at The Edge of Slab for Tested Specimens Of Phase I

The load-deflection curves for the tested specimens from the start of applying the load, and up to failure for all groups are plotted in Figures 14 to 16 and cracking load P_{cr}, ultimate load P_u, ultimate deflection Δ_u and toughness for all tested specimens are shown in Table 3.

It was seen from load-deflection relationship of specimens of group GIM that; the tested specimens illustrated linear deflection behavior before cracking. After cracking occurred, with the loading increased as stiffness was reduced. For specimens GIM-2, GIM-3, and GIM-4, lower values of the ultimate load and deflection were noticed compared with the control specimen GIM-1. It is obvious from the results that; control specimen GIM-1 possesses the highest load resistance among all specimens of this group. In the case of an increase in the percentage of malposition ratio from 20% to 40%, the ratio of decrease in the ultimate load is 21.87%, while when this percentage

reached 60%, the rate of decrease in the maximum loading is equal to 35.93% and when the percentage increase in the malposition in the reinforcement of slab to 80%, the decrease in the maximum load is 42.18%.
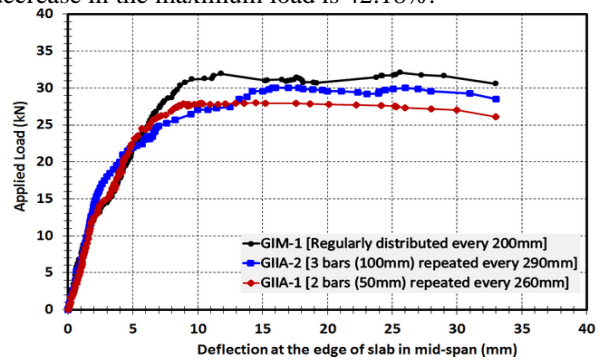
Figure 15 Comparison between the tested specimens of group GII
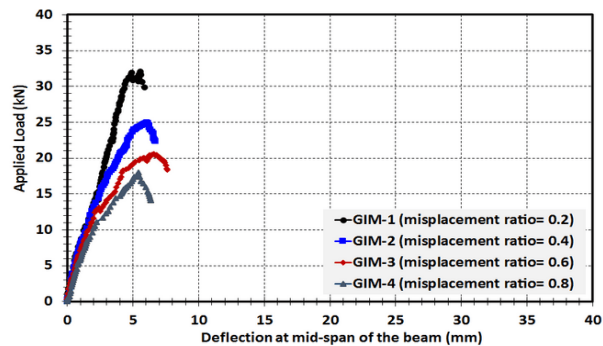
Figure 16 Comparison between the tested specimens of group GIII

Thus, it can be concluded from the previous results that, the rate of increase for the ratio of slab reinforcement malposition was less than the ultimate load value of the tested specimen, but the rate of decrease in the ultimate load was not the same as the rate of increase in the percentage of the wrong placement in slab reinforcement. The area under the load-deflection relationship up to failure is called toughness. Toughness is the ability of the material to withstand or absorb mechanical energy as shown in Table 3. It can be concluded from comparison of group GIM that; the rate of increase for the ratio of slab reinforcement malposition was less than the ultimate load value of the tested specimen, but the rate of decrease in the ultimate load was not the same as the rate of increase in the percentage of the wrong placement in slab reinforcement. A lower position of the reinforcement leads to a lower bending

moment capacity of the slab and can also lead to a brittle behavior in case of collapse.
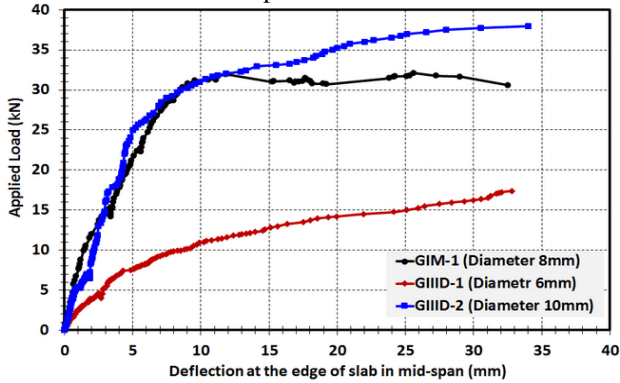
Figure 17 Comparison between the tested specimens of group GI

It was found from the results of group GIIA that; the control specimen GIM-1 recorded an increase of 4.68% and 12.5% in the ultimate load over specimens GIIA-1 and GIIA-2, respectively. However, the decrease in the load capacity with the increase in irregularity of slab reinforcement (large spacing between reinforcing bars) was higher. Specimen GIIA-1 recorded a decrease of 5.71% and the last specimen GIIA-2 recorded an increase of 5.14% in the deflection at ultimate load, respectively. It can be concluded that well-arranged distribution of reinforcement improves the ductile behavior of the slab and reduces the corresponding deflections. Meanwhile, the eccentricity of main steel creates a sort of non-uniform stress distribution over the section and accelerates the failure.

The comparison of group GIIID showed that the use of 10mm diameter in the reinforcement of the slab exhibited high resistance to loads while on the contrary, the 6mm diameter reinforcement offered a weak resistance to the loads affecting the slab. Load-deflection responses for specimens GIM-1 and GIIID-2 showed approximately the same trend, and no significant difference was observed at low loading level, while the third specimen GIIID-1 exhibited a significant difference in values of the deflection from the beginning of loading. From the test results of group GIII, it is concluded that an increase in the diameter of slab reinforcement while keeping reinforcement ratio constant enhanced the behavior of T-beam to withstand the loads and increased the ductility of the T-beams. It also improves the efficiency of T-beam section under the loading effect, the minimum bar diameter for the reinforcement of slab is 8mm because the 6mm diameter reinforcement was found to be weak in resisting the loads.

Load-Deflection Behavior at Mid-Span of The Attached Beam for Specimens of Phase

Figure 17 shows load-deflection relationship at mid-span of the attached beams for group GIM. It is apparent that the shape of the load-deflection curves in the elastic region before cracking is the same for the all specimens. However, it appears that after cracking, both specimens GIM-1 and GIM-2 produced higher values of deflection than specimens GIM-3 and GIM-4 for the same level of loading. The maximum deflection of specimens GIM-1, GIM-2, GIM-3, and GIM-4 was 5.9mm, 6.7mm, 7.55mm, and 6.3mm, respectively at the failure load. It can be said that the ill

effect from the malposition of slab reinforcement is more serious on the behavior of slab and the attached beam than the correct place for reinforcing steel for the slab.
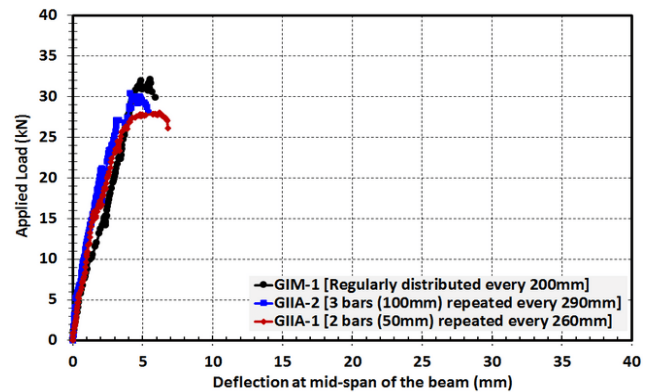
Figure 18 Comparison between the tested specimens of group GII
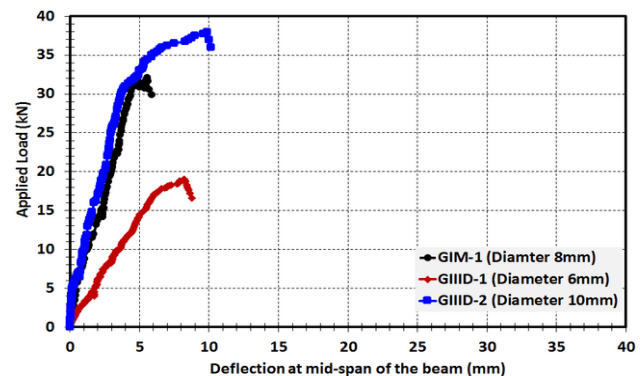
Figure 19 Comparison between the tested specimens of group GIII

The load-deflection curves for specimens of group GIIA are shown in Figure 18. There is no significant difference between three specimens in the values of deflection, especially at the beginning of loading before the initiation of cracks. The maximum deflection for the specimens GIM-1, GIIA-1 and GIIA-2 at the failure load was 5.90mm, 6.80mm, and 5.75mm, respectively. It is evident that the irregularity of the reinforcement of slab does not have any significant effect on the efficiency of a concrete beam connected with the slab. Furthermore, the beam attached to slab was not significantly affected by the irregularity of the shape of slab reinforcement.

Figure 19 shows the comparison between specimens of group GIIID. It was found that the use of 10mm diameter in reinforcing the slab in T-section significantly improved the flexural behavior of the slab to resist the load. Thus, the behavior of the beam connected to the slab improved to withstand the loads. Also, there is no clear difference between the behavior of specimens GIM-1 and GIIID-2 with slab reinforcement with diameters 8mm and 10mm in load-deflection values. The maximum deflection value for the beam at the failure was 5.9mm, 8.75mm and 10.25mm for specimens GIM-1, GIIID-1, and GIIID-2, respectively. Specimen GIIID-2 demonstrated higher deflection than specimen GIM-1 and GIIID-1 where this specimen reinforced the slab with a diameter of 10mm, showed the beam connected to the slab a high resistance to loads. Therefore, it is preferable to use 10mm or higher diameter in reinforcing the slabs.
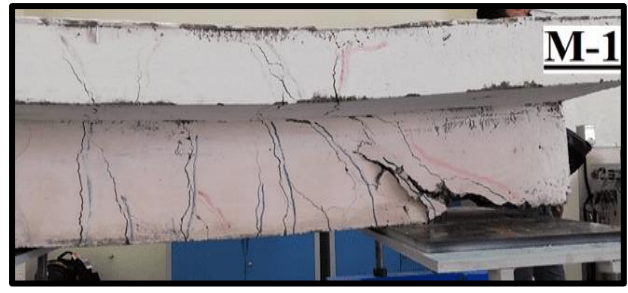
<div align="center">(a)   (b)</div>

<div align="center">Figure 20 (a) Cracking pattern of specimen M-1 (b) Crushing of concrete at the right support of specimen M-1</div>

B. RESULTS AND DISCUSSION FOR LOADING THE SLAB AND BEAM SIMULTANEOUSLY (T-BEAM) WITH TWO CONCENTRATED LOADS

Crack Pattern and Failure Mechanism for Specimens of Phase II

The formation of cracks at every stage of loading is marked on the test T-beams. At an early stage of its loading history, concrete was cracked firstly because its weak in tension. It can be seen from the cracking patterns that the presence of breadth of slab in resisting of loads with the attached beam affected on the cracks initiation and propagation at different degrees from the applied loads. The initial flexural cracks occurred in the flexural region (maximum bending moment) at mid span of the T-beam between points loads. These cracks were perpendicular to the direction of the maximum principal tensile stress trend to the direction of the loading regions. Specimens M-1 and A-1 have shown that the first crack form at a nearly identical load level, which was about 40kN and 43kN, respectively whereas for remaining specimen D-1, the first crack happened at load level equal to 55kN.

With increasing the load level, shear cracks observed at the supports and spread diagonally towards the loading regions. However, the failure modes were a flexural failure. The cracks continued growing in the attached beam and these cracks extended to the bottom of the slab. Thus, these flexural cracks penetrate deeper in the slab of the T-section beam (compression zone) and these cracks become widened due to the effect of bending stresses. These cracks penetrated upward as the load increased and new cracks propagated toward the points load. As the loaded increases in specimen M-1, the cracks under the right point load have deeply penetrated to the compression zone resulting in complete flexural failure and crushing of concrete occurred at the right support location as shown in Figure 20. While in specimens A-1 and D-1, the cracks were concentrated in the central region from T-section beam and the failure took place due to the concentration of tension stresses in this region as illustrated in Figure 21 and 22. This type of failure was classified as a complete flexural failure except specimen C-1 and ultimate load happened in specimens M-1, A-1 and D-1 at load level equal to 105kN, 115kN and 150kN, respectively.
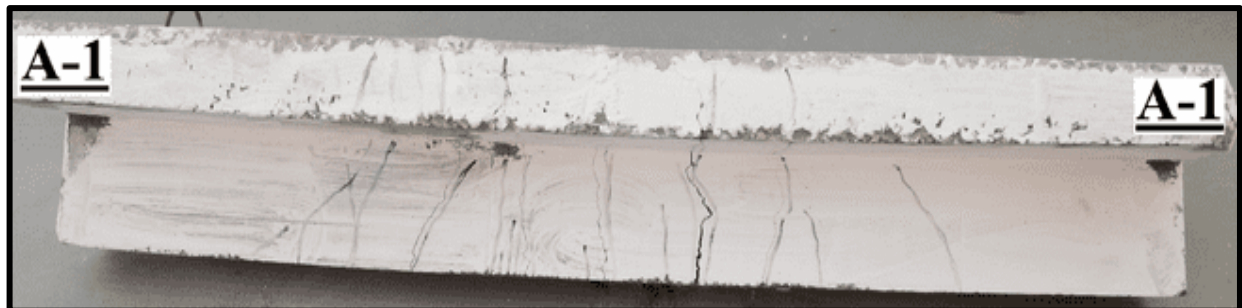
<div align="center">(a)</div>
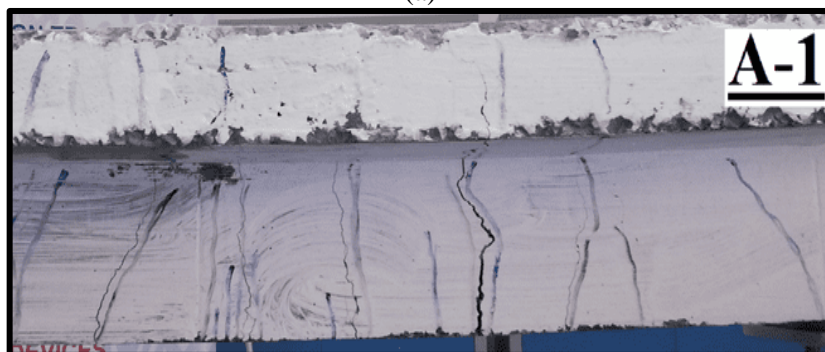
<div align="center">(b)</div>

<div align="center">Figure 21 (a) Cracking patterns of specimen A-1 (b) cracks concentrated at mid span for specimen A-1</div>

(a)

(b)

Figure 22 (a) Cracking patterns of specimen D-1 (b) Cracks concentrated at mid-span for specimen D-1

(a)

(b)

Figure 23 (a). Cracks pattern for specimen GIM-5 (b) Cracking pattern of specimen GIM-5 (mid-span)

For specimen GIM-5: The appearance of the tested specimen after loading is shown in Figure 23 (a) and (b). The specimen GIM-5 showed the typical cracking behavior of under reinforced concrete simple beam and failed in ductile flexural tension. At early loading levels, vertical cracks appeared in region of shear towards loading points at load equal to 8.80kN. Upon increasing the load, the cracks started at maximum tensile stresses (region of maximum bending moment). With increasing the load, the number, width, and extensions towards the compression zone of the cracks increased. Cracks concentrated at section of the maximum bending moment and at later stages of loading, the failure occurred in the middle third of the beam span. However, at load equal to 45kN, the specimen failed with ductile mode failure when the load reaches its peak value.

Table 4 Summary of results for specimens of phase II

Specimen Notation	Cracking Load (P_{cr}) (kN)	Ultimate Load (P_u) (kN)	Ultimate deflection Δ_u (mm)	$\dfrac{P_{cr}}{P_u}$	$\dfrac{P_u}{P_u \text{ (M-1)}}$	Toughness (kN.mm)
M-1	40	105	24	0.381	1	1956.05
A-1	43	115	24	0.373	1.095	2395.3
D-1	55	150	26	0.367	1.428	3315.88

Load-Deflection Behavior at The Edge of Slab for Tested Specimens of Phase II

Figure 24 represents the applied load versus deflection curves at the end of slab in mid-span for the studied specimens of phase II. Loading was affected on the entire width of the slab and the attached beam and loading was affected gradually on these specimens. The cracking load P_{cr}, ultimate load P_u, ultimate deflection Δ_u and toughness for all specimens are presented in Table 4.
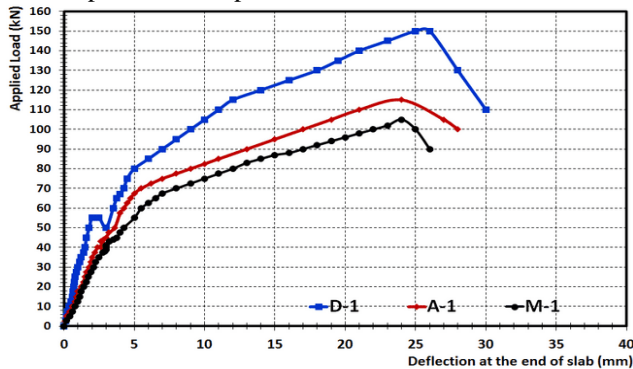
Figure 24 Comparison between the tested specimens of phase II

From the relation between load and deflection of specimens of phase II, it was observed that; these curves were composed of three distinguished regions namely, pre-cracking stage, post cracking stage and post serviceability cracking stage. At pre-cracking stage, all T-section beams have displayed similar behavior and the applied loads are directly proportional to the value of deflections at the end of slab in mid-span. This means that the whole concrete T-section beam is effective in resisting deflection, which affected by applied load.

Therefore, the pre-cracking segment of load deflection curve is defined as full elastic behavior for all specimens tested here. When the load on the test T-section beams is gradually increased beyond the first crack to the ultimate load, the behavior of specimens A-1 and M-1 changed slightly in to a post-cracking stage. This variation between specimens A-1 and M-1 was due to the fact that non-distribution of slab reinforcement regularly and concentrate the reinforcing bars below the loading regions of specimen A-1 was strongly contributed in this a slight increase in the ultimate load of specimen A-1. While behavior of specimen D-1 varied significantly from specimens A-1 and M-1, specimen D-1 has shown better load deflection behavior than specimens A-1 and M-1.

At post-cracking ultimate load stage, the formation of flexural cracks in T-section beams reduced the flexural stiffness of the T- beam section making the load-deflection curve less steep in this region than in the pre-cracking stage segment. By increasing further load beyond the ultimate point, the T-section beams presented substantial loss in their stiffness because of the extensive cracking penetrating to the compression zone and the load deflection curve tend to be flatter. The small increase in the applied load resulted in large amount of deflection.

From the previous results, it can be concluded that; reinforced concrete T-section beams show significant increasing the flexural capacity of beams cracked in flexural, compared to other loading case. The presence of slab in resisting load with the attached beam showed increase in the maximum applied load prior to failure, and reduced the short term deflection of the studied T-beams to different degrees. The ultimate load of specimen M-1 was 105kN, decreasing by 9.50%, 42.85% lower than the load capacity of specimens A-1 and D-1, respectively. The use of 10 mm diameter in reinforcement of the slab has enhanced the serviceability of T-beams affecting loads compared to the specimens which used the diameter 8mm in slab reinforcement, where this specimen recorded the highest resistance to loads.
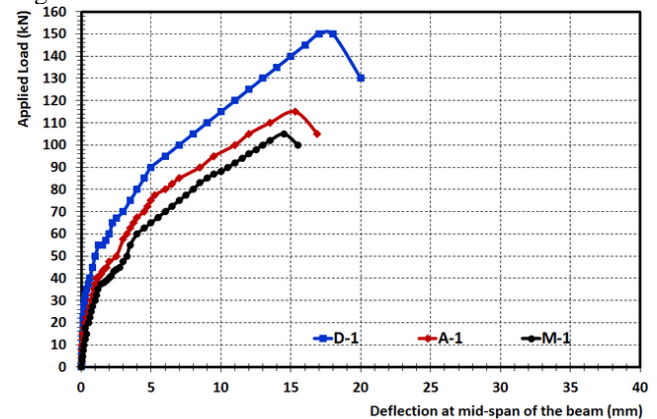
Figure 25 Comparison between the tested specimens of phase II

Load-Deflection Behavior at Mid-Span of The Attached Beam for Specimens of Phase II

The measured values of maximum deflection at mid span for all tested beams are plotted against the applied load from

Table 5 Summary of deflection results for specimens of phase II

Specimen Notation	Ultimate Load (P_u) (kN)	Ultimate deflection Δ_u (mm) at the edge of slab	Ultimate deflection Δ_u (mm) at mid-span of the beam
M-1	105	24	14.50
A-1	115	24	15.30
D-1	150	26	18.60

Table 6. Summary of the results for specimens M-1, GIM-1 and GIM-5

Specimen Notation	Cracking Load (P_{cr}) (kN)	Ultimate Load (P_u) (kN)	Ultimate deflection Δ_u (mm)	$\dfrac{P_{cr}}{P_u}$	$\dfrac{P_u}{P_u \text{ (Control)}}$	Toughness (kN.mm)
M-1	40	105	14.5	0.381	2.1875	1311.88
GIM-1 (Control)	9	48	32	0.1875	1	1287.61
GIM-5 (Beam only)	8.8	45	31	0.195	0.9375	897.08

starting to failure as shown in Figure 25. Table 5 summarized deflection results for specimens of phase II. It can be observed from the previous comparison that the presence of slab in resisting loads with the attached beam affected the value of deflection at different applied loads prior to failure at different stages. Before cracking, the behavior of specimens was similar but after cracking initiated the specimen D-1 showed lower deflection and higher load among other specimens while both specimens A-1 and M-1 produced the same values of deflection approximately. The maximum deflection of specimens M-1, A-1 and D-1 was 14.50mm, 15.30mm and 18.60mm, respectively at the ultimate load.

From the previous results it could be said that participation of the slab in resisting loads with the attached beam improved resistance of T-section beams to the affecting loads and reduced the value of deflection in all specimens. The existence of the slab increased the load capacity of the T-beam. Moreover, it is preferred that the minimum diameter of bar used in main reinforcement of slab should not less than 10 mm because this diameter enhanced the resistance of slab to affected loads.

Load-Deflection Behavior at Mid-Span of The Beam for specimens GIM-1, M-1, and GIM-5

The total applied load and the vertical deflection measured at mid-span of the attached beam for specimens GIM-1, M-1 and GIM-5 are shown in Fig. 26. It can be noted that the tested specimens demonstrated linear load-deflection behavior before cracking and it is easily noted that at about 25% of the ultimate load and there were no evident of difference in deflection between specimens GIM-1 and GIM-5 except the specimen M-1, which behaved differently than the other specimens from the start of loading. However, after the beginning of the first crack, the effect of existence of slab (flange) in specimens GIM-5 and GIM-1 was clear in the form of more deflection at the same load level for specimen without flange (rectangular beam). The behavior of specimens GIM-5 and GIM-1 were close, but the GIM-1 was higher in the deflection values, indicating that the presence of slab (flange) to the resistance of the highest loading effect compared to the specimen that does not have a slab (flange). Table 6 summarizes the results between three specimens M-1, GIM-1 and GIM-5.

It is clear from previous results that; the maximum load of specimen GIM-5 is less than the ultimate load of specimens GIM-1 and M-1 by 6.25% and 133.33%, respectively. The cracking load of the specimen GIM-1 is greater than that of specimen GIM-5 and lower than specimen M-1. The toughness was increased with the increase of the stiffness of specimen GIM-1 by 30.32% than

specimen GIM-5 while decrease approximately by 2% than specimen M-1.

This indicates that the first specimen M-1 (loading slab and beam simultaneously) (T-section beam) and the second specimen GIM-1 (loading the attached beam only after cracks occurred in the slab) showed higher resistance and performance in the load resistance compared to the specimen that does not contain the slab (rectangular beam only). It was confirmed from experimental tests that T-beams were significantly influenced by existence of the flange (slab) in resisting of loads. Flexural capacity of T-beams was higher than for rectangular beams where T beams have a higher moment of inertia than rectangular beams and thus flexural can be resisted more effectively. Hence from the previous discussion, it can be concluded that, T-beams are more efficient than rectangular beams where part of slab contributes to the resistance of the loads.

CONCLUSIONS

Based on the experimental test results obtained in this investigation, the following conclusions can be drawn:

- A lower position of the reinforcement can be caused by insufficient support of the reinforcement during the execution and the pouring of the concrete, leading to a lower bending moment capacity of the slab and can also lead to a brittle behavior in case of collapse.
- Malposition of slab reinforcement ratio increased from 20% to 40%, the ratio of decrease in the ultimate load of 21.87%, while when this percentage reached 60%, the rate of decrease in the maximum loading equal to 35.93% and when the percentage increase in the place of misplacement in the reinforcement of slab to 80%, the decrease in the maximum load was 42.18%.
- The toughness decreased with the increase in the ratio of misplacement of reinforcing bars of slab where the decrease in toughness was 71.52%, 60.11%, and 50.57% for malposition ratio (tmis./ts) for reinforcing bars of slab equal to 0.40, 0.60 and 0.80%, respectively.
- The regularity of reinforcement of slab plays an important role in the resistance of slab against the loads. It was found that the control specimen GIM-1 recorded an increase of 4.68% and 12.5% in the ultimate load over specimens GIIA-1 and GIIA-2, respectively. The toughness of these specimens GIM-1, GIIA-1 and GIIA-2 is found to be 981.21kN.mm, 828.08kN.mm and 973kN.mm, respectively. However, the decrease in the load capacity with the increase in irregularity of slab reinforcement (large spacing between reinforcing bars) was higher.
- Well-arranged distribution of slab reinforcement improves the ductile behavior and reduces the

corresponding deflections. Meanwhile, eccentricity of main steel creates a sort of non-uniform stress distribution over the section and accelerates the failure.

- The increasing of the diameter of slab reinforcement while keeping reinforcement ratio constant enhanced the behavior of T-beam to withstand the loads and increased the ductility of the T-beams. Specimen GIIID-2 showed 143.9% increase in ductility compared to control specimen while specimen GIIID-1 decreases 61.82% lower the control specimen.

- To improve the efficiency of T-beam section under the loading effect, the minimum bar diameter for the reinforcement of slab is 8mm because the 6mm diameter reinforcement was found to be weak in resistance to the loads. The reinforcement of slab with diameter 10mm helped the slab to withstand more loads and delay the occurrence of cracking.

- The ultimate load of specimen M-1 was 105kN, which is decreasing by 9.50%, 42.85% lower than the load capacity of specimens A-1 and D-1, respectively. In addition, the toughness value of specimen M-1 was decreased by 22.46% and 69.52% lower than specimens A-1 and D-1, respectively.

- The use of 10 mm diameter in reinforcement of the slab has enhanced the serviceability of T-beams for affecting loads compared to the specimens which used the diameter 8mm in slab reinforcement, where this specimen recorded the highest resistance to loads.

- T-beams were significantly influenced by existence of the flange (slab) in resisting of loads. Flexural capacity of T-beams were higher than for rectangular beams. T-beams are more efficient than rectangular beams where part of slab contributes to the resistance of the loads.

- The specimen with a slab (flange) has a high performance in resisting the loads affecting compared to the specimen does not have a slab (rectangular beam). The existence of the flange in the T-section that resulted in higher stiffness than the R-section.

- The maximum load of specimen GIM-5 is less than the ultimate load of specimens GIM-1 and M-1 by 6.25% and 133.33%, respectively. The toughness was increased with the increase of the stiffness of specimen GIM-1 by 30.32% than specimen GIM-5 while decrease approximately by 2% than specimen M-1.

- Flexural capacity of T-beams were higher than for rectangular beams where T beams have a higher moment of inertia than rectangular beams and thus flexural can be resisted more effectively.

- The presence of higher reinforcement area in T-beam section compared to rectangular beam section increased the strain capacity of the beam while the strain in main reinforcement of the T-concrete beam reached to the yielding range through the testing of slab. The section of concrete slab did not change from T-section to rectangular section and the slab still resisted the effecting loads.

REFERENCES

[1] N. V. Bagdiya and S. Wadalkar. "Review paper on construction defects". *IOSR Journal of Mechanical and Civil Engineering (IOSR-JMCE)*, vol. 12, no. 2, pp. 88-91, 2015

[2] E. C. P., *Egyptian code of practice for design and construction of reinforced concrete structures (ECCS203-2007)*. (Egypt: Housing and Building Research Center). 2007

[3] A. C. Institute. "Causes, evaluation and repair of cracks in concrete structures (ACI 224.1R-93)". *American Concrete Institute Journal,* pp. 1-22, 1993

[4] T. M. Elrakib and A. I. Arafa, "Experimental evaluation of the common defects in the execution of reinforced concrete beams under flexural loading". *HBRC Journal*, vol. 8, pp. 47-57, 2012.

[5] J. E. Afunaya, "Assessment of construction errors in reinforced concrete beams". *International Journal of Civil and Structural Engineering*, vol. 6, no. 1, pp. 105-118, 2015

[6] E. A. Bayoumi, M. A. Eliwa and A. G. Asran. "Assessment of construction errors in execution of reinforced concrete T-beams". *Journal of Advanced Civil Engineering Practice and Research*, vol. 6, no. 2, pp. 103-114, 2018

[7] A. K. Baiburin. "Errors, defects and safety control at construction stage". *Procedia Engineering*, vol. 206, pp. 807-813, 2017

[8] C. R. R. González, M. F. Ruiz, "Influence of flanges on the shear-carrying capacity of reinforced concrete beams without web reinforcement". *Structural Concrete Journal*, vol. 18, no. 5, pp. 720-732, 2017

[9] Z. Yannian, X. Jun and W. Liu. "Experimental study on RC T-section beams strengthened with bottom steel plates". *Jordan Journal of Civil Engineering*, vol. 12, no. 3, pp. 502-515, 2018

[10] P. Eswaramoorthi, P. S. Prabhu and P. Magudeaswaran. "Experimental study of reinforced concrete continuous rectangular and flanged beams at support region". *International Journal of Civil Engineering and Technology*, vol. 8, no. 7, pp. 706-713, 2017

[11] A. G. Asran, M. A. Eliwa and E. A. Bayoumi, "Performance evaluation of RC T-beam sections made with the common defects under flexural loading". *Journal of Civil Engineering and Structures*, vol. 2, no. 4, pp. 18-36, 2018

[12] E. A. Bayoumi, A. G. Asran and M. A. Eliwa, "Mechanical performance of construction errors in implementation of T-reinforced concrete beams". *Jordan Journal of Civil Engineering*, vol. 13, no. 1, pp. 97-112, 2019

[13] I. G. Shaaban, M. Saidani, M. F. Nuruddin, A. B. Malkawi and T. S. Mustafa. "Serviceability behavior of normal strength concrete and high strength concrete T-beams". *European Journal of Materials Science and Engineering*. vol. 2, no. 4, pp. 99-110, 2017

[14] A. G. Asran, M. A. Eliwa, M. A. Alkersh and E. A. Bayoumi, "An assessment of the effect of construction

errors during the implementation of RC T-Beams". *The Journal of Engineering Research (TJER)*, vol. 16, no. 2, pp. 103-114, 2019

[15] R. Thamrin, J. Tanjung, R. Aryanti, O. F. Nur and A. Devinus. "Shear strength of reinforced concrete T-beams without stirrups". *Journal of Engineering Science and Technology*, vol. 11, no. 4, pp. 548-562, 2016

[16] A. H. Zaher, W. M. Montaser, and A. K. Elshenawy. "Shear behavior of light weight concrete T –beams". *International Journal of Emerging Technology and Advanced Engineering*, vol. 5, no. 12, 2015

[17] R. Al-Mahaidi, G. Taplin, and C. Giaccio. "Experimental study on the effect of flange geometry on the shear strength of reinforced concrete T-beams subjected to concentrated loads". *Canadian Journal of Civil Engineering*, vol. 29, no.6, pp. 911-918, 2011

[18] D. B. Ghailan. T-beam behavior in flexure with different layers of concrete in web and flange. *Kufa Journal of Engineering*, vol. 2, no. 1, pp. 53-61, 2010

[19] W. Pansuk and Y. Sato. "Shear mechanism of reinforced concrete T-beams with stirrup". *Journal of Advanced Concrete Technology*. vol. 5, no. 3, pp. 395-408, 2007